FIELD-OF-VIEW, DETECTION RANGE, AND FALSE ALARM TRADE-OFFS IN VISION-BASED AIRCRAFT DETECTION

John Lai*, Jason J. Ford*, Luis Mejias*, Alex Wainwright*, Peter O'Shea*, Rodney Walker*[1]
***Australian Research Centre for Aerospace Automation (ARCAA)**
Queensland University of Technology, GPO Box 2434, Brisbane Queensland 4001, Australia
{js.lai, j2.ford, luis.mejias, alexander.wainwright, pj.oshea, ra.walker}@qut.edu.au

Keywords: *Sense-and-avoid, computer vision, collision avoidance*

Abstract

This paper presents a survey of previously presented vision-based aircraft detection flight test, and then presents new flight test results examining the impact of camera field-of-view choice on the detection range and false alarm rate characteristics of a vision-based aircraft detection technique. Using data collected from approaching aircraft, we examine the impact of camera field-of-view choice and confirm that, when aiming for similar levels of detection confidence, an improvement in detection range can be obtained by choosing a smaller effective field-of-view (in terms of degrees per pixel).

1 Introduction

Over the last 5 years, our organization has investigated a number of key technology issues related to the integration of unmanned airborne systems (UAS) into the national airspace, for example see [1–13]. Amongst these issues, one of the more important is the automation and replication of the human pilot see-and-avoid capability [14, 15]. The lack of certified sense-and-avoid technology (the automated version of see-and-avoid) has been previously identified as a key barrier to further utilization of Unmanned Aerial System (UAS) [16, 17]. A sense-and-avoid solution based on machine vision has been suggested as one of the most promising approaches for gaining regulatory approval [18]. This opportunity motivates us to examine some important performance characteristics of vision-based aircraft detection technology.

The authors of this paper has been developing vision-based collision avoidance technology since 2005, see [1–13]. During our investigations we have evolved technological capability from simulation and ground based testing [1–3], through hardware implementations considerations [5, 6], via UAS-on-UAS flight tests [7] and aircraft-on-aircraft flight testing [9], to closed-loop automated collision avoidance flight testing (between two aircraft) [11, 12]. During this period of investigation, we conducted trade-studies of various algorithm choices, see details [1–4, 7, 10], leading to the conclusions that morphology hidden Markov model algorithms are the current state of the art for this application, see a detailed description of such algorithms in [7, 13]. We have also conducted integrated airspace flight tests (involving a mixed airspace of rotorcraft UAV, fixed-wing UAV and manned aircraft) [8].

The first contribution of this paper is to present a suvery of the reported ground and airborne captured data tests related to the performance of vision-based aircraft detection approaches. This survey suggests that the initial feasibility of vision-based target detection has been successfully demonstrated (confirming the observations from our own testing program, as reported in [1, 7, 9, 11, 12]), but has also identified a number of important practical issues (such as

[1] Rodney Walker died October 2011.

false targets arising from cloud backgrounds and compensation for platform vibrations and aerodynamic disturbances [7]).

The second contribution of this paper is to consider the critical system design trade-offs of: field-of-view, detection range, and false alarm performance (on the basis of a practical real-time target detection approach that exploits hidden Markov model and image morphology filtering concepts). In our empirical study a ground based camera with multiple lens configurations was used to collect head-on-approaching target images for evaluation of detection ranges. Unlike previous studies, we also captured a large corpus of non-target background images to assess false alarm performance down to a resolution of approximately 1 per hour (continuing work aiming for low-false alarm rates is outlined in [9]). Our results are presented in terms of receiver operating characteristic (ROC) curves and qualified by a detection confidence measure related to signal-to-noise ratio (SNR) quantities.

2 Survey of a Decade of Vision Based Aircraft Detection Experiments

An examination of the literature related to image-based aircraft detection technology identified 15 papers during the period 1999 to 2011 that reported flight or ground-based data collection experiments (we found no published studies before 1999). Of these 15 papers, 11 studies reported sufficient information to determine at least one of the following measures of detection performance: detection distance (reported distances ranged from 18.5 km to 0.89 km), detection rate (ranging from 35.7% to 100%), and false alarm rate (ranging from 2.62 to 0.0004 false alarms per frame). The performance of the detection approaches from these 11 studies are summarised in Tables 1 and 2 (this includes 3 studies involving data collected from a ground-based vision sensor and 8 studies involving data collected from an airborne platform). For comparison purposes, we will also include 2 studies that have reported detection distance results for human observers.

The 11 identified vision-based aircraft detection experiments reported using a variety of: image resolutions (ranging from 646 x 468 [27] to 2048 x 1024 [24]), camera fields-of-view (ranging from 13° x 9.75° [27] to 62.3° x 39.5° [7]), and data collection platforms (ranging from Boeing 737 aircraft [27] to UAS [7], and also some stationary ground configurations). The vision detection algorithms investigated in these 11 studies can be characterised as involving three types of processing stages: 1) egomotion compensation; 2) image processing pre-filtering; and 3) temporal filtering. Not every reported detection algorithm involved all 3 processing stages (but at least one of the stages was reported in each paper examined in this survey). The reported egomotion compensation techniques included: inertial-based compensation [23, 27] and image-based compensation [7]. The reported image processing pre-filtering stages included use of: morphological filtering [1], optical flow [24–27], low-stop filtering [23], object detection [28] and non-maximal suppression [23, 28]. The reported temporal filtering stages included use of: Kalman filters [23, 25], dynamic programming [1, 7], and hidden Markov model filters [7].

We have summarised the performance claims of the 11 candidate detection approaches in Tables 1 and 2. These tables list the reported maximum detection range (with track consistency percentage, if provided), and false alarm (FA) rate expressed in FA per frame (with measurement precision, as determined from the number of frames used in FA calculations, where adequate information was provided). We have also provided information about the angular resolution of the vision sensor and the wing span of the target aircraft. To facilitate comparisons with experiments involving a human observer, we have assumed the human eye to possess an equivalent angular resolution value of 60°/pixel (human visual acuity is reported in [29] as 60°/cycle, where a cycle can roughly be interpreted as the human vision equivalent of a pixel). However, we acknowledge that this nominal human eye angular resolution value neither accounts for the many subtleties of the human vision system nor describes variations between particular individu-

als. Finally, to allow comparison between systems with different fields-of-view, we have introduced a detection **effectiveness** measure, inspired by [30], which is defined as the ratio of detection range to pixels per degree, divided by the target aircraft wingspan. The purpose of this effectiveness metric is to measure how effectively the angular resolution is used (higher numbers correspond to better use).

2.1 Current Gaps and Future Requirements as Identified in the Survey

Collectively, the surveyed experiments clearly illustrate the possibility of using vision-based aircraft detection techniques to detect potential airborne collisions at sufficient ranges to allow safe avoidance action. However, amongst the surveyed experiments, there was significant inconsistency and an overall lack of detail provided about false alarm performance. Less than half of the currently reported studies provided an adequate characterisation of false alarm performance. Standard detection versus false alarm performance characterisation tools, such as Receiver Operating Characteristic (ROC) curves (or similar), were only provided in five studies [19, 23,27,28]. Due to this general lack of false alarm performance characterisation (corresponding to false alarm rates low enough for practical use), there is scope for further research in this domain before vision-based detection technology can be considered well understood (and we are investigating this false alarm issue in ongoing research, as preliminarily reported in [9]).

In the remainder of this paper, we will investigate the tradeoffs between field-of-view, detection range, and false alarm susceptibility.

3 Methodology for Evaluating Field-of-View issues

In the following, we will use an empirical approach to evaluate the impact of changing the field-of-view of the sensor in a vision-based target detection system. Within that empirical approach, we will use a morphological-HMM target detection algorithm, see [7, 13], as our baseline system (this will remain constant through all the tests reported here). Before presenting our result, this section describes the data collection approach, the processing algorithm, and performance measures used for characterisation.

Table 3 Data collection lens types

Lens Model	Computar **H0514-MP**	Computar **M1614-MP**	Fujinon **HF50HA-1B**
Focal Length	5mm	16mm	50mm
Field-of-View (H×V, degrees)	$51.4° \times 39.5°$	$16.9° \times 12.7°$	$5.5° \times 4.1°$
Degrees/pixel (1024×768 pixel image)	5.08×10^{-2}	1.65×10^{-2}	5.4×10^{-3}

3.1 Data Collection

We used a ground based Basler Scout series camera (scA1300-32fc) in combination with the lenses shown in Table 3 to capture image data at 25Hz with a resolution of 1024-by-768 pixels. With each lens we captured images of a Cessna 172 aircraft against a clear sky background approaching the camera from a head-on geometry (roughly replicating what would be observed in an airborne head-on collision situation). State data logged on the target aircraft enabled calculation of detection ranges post-flight. Furthermore, with the M1614-MP lens we also collected 1.1 hours (approximately 1×10^5 image frames) of non-target clear sky background data to facilitate characterisation of false alarm performance.

3.2 Detection Algorithm

Detection was on the basis of the morphological-HMM dim-target detection algorithm described in [7, 13]. As an example of the difficulty of the problem, Figure 1 illustrates the benefits of the image morphology operation for dim target enhancement. The top image is a cropped raw image frame centered on a dim target aircraft, and the corresponding output after morphological filtering is shown below. The HMM temporal filtering is used after this morphological filtering stage to reinforce features that persist in the image (as

Table 1 Vision based aircraft detection performance in ground tests (sorted by detection effectiveness).

Author	(year)	Target	Wingspan	Resolution in pixel/○	Range (% reliability)		FA/frame		Effectiveness
Carnie	(2006) [1]	Cessna 172[2]	11.00 m	60, see [29] (human)	4.9 km (human)	(n/a)	n/a		0.0074 (human)
Dey	(2009) [19]	Piper Archer II	10.82 m	43	8.05 km	(98%)	0.02	±?	0.0173
Lai	(this paper)	Cessna 172	11.00 m	60	2.625 km	(n/a)	0.005	±0.00001	0.00398
Carnie	(2006) [1]	Cessna 172	11.00 m	60	6 km	(n/a)	2.62	±0.005	n/a

Table 2 Vision based aircraft detection performance in airborne tests (sorted by detection effectiveness).

Author	(year)	On-board processing	Target	Wingspan	Resolution in pixel/○	Range (% reliability)		FA/frame		Effectiveness
Kephart	(2010) [30]	n/a	Piper Warrior	10.67 m	60 (human)	3.759 (human)	(n/a)	n/a		0.0059 (human)
McCalmont	(2007) [24]	Yes	King Air	≈14-16 m	35	18.520 km	(n/a)	n/a		0.0331
Lai	(2011) [7]	Yes	Boomerang 60	2.1 m	20	0.893 km	(n/a)	n/a		0.0213
Utt	(2004) [25]	Yes	Beech Bonanza	10.21 m	35	7.408 km	(≈100%)	0.0005	±?	0.0207
McCalmont	(2005) [26]	Yes	Beech Bonanza	10.21 m	35	5.556 km	(n/a)	n/a		0.0155
Gandhi	(2003) [23]	No	Beech King Air	16.61 m	105	10.0 km	(35.7%)	0.0	±0.0024	0.00573
McCandless	(1999) [27]	No	Beech King Air	16.61 m	50	2.222 km	(82%)	0.0	±0.0037	0.00268
Petridis	(2008) [28]	No	Beech King Air	16.61 m	50	n/a	(89.67%)	3.88	±0.0004	n/a
Petridis	(2008) [28]	No	Beech King Air	16.61 m	50	n/a	(98.27%)	0.0487	±0.0016	n/a

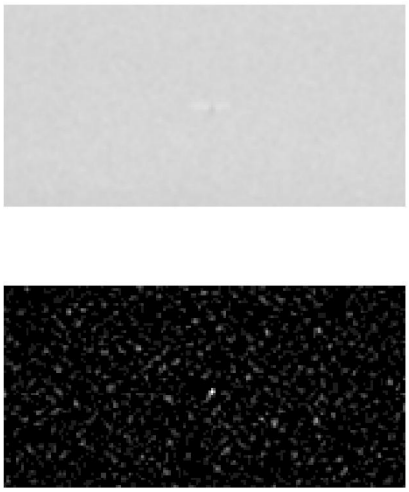

Fig. 1 Dim target image enhancement via morphological filtering. The top image is centered on a dim target aircraft (the target is very difficult to detect), and the image below shows the output after morphological filtering (the target corresponds to the brightest spot).

expected of features corresponding to the true target).

3.3 Performance Metrics

In this study we will use ROC curves and a detection confidence measure based on SNR quantities to characterise detection performance. Our ROC curves will illustrate detection range versus false alarm rate trade-offs, while detection confidence will be indicated by the ΔDSNR quantity that has been previously used in [7] (and is conceptually similar to the DTMB statistic in [22]). The ΔDSNR quantity is given by:

$$\Delta\text{DSNR} = 20\log_{10}\left(\frac{P^T}{P^F}\right)\text{dB}, \qquad (1)$$

where P^T is the maximum target pixel intensity at the filtering output and P^F is the highest non-target pixel response at the filtering output. Strong filter responses away from the true target location will tend to lower the ΔDSNR value.

4 Results

4.1 Field-of-View Comparison

Figure 2 shows two curves illustrating the trade-off between camera field-of-view (FOV) and de-

[2]Target information obtained from personal correspondence, July 2011.

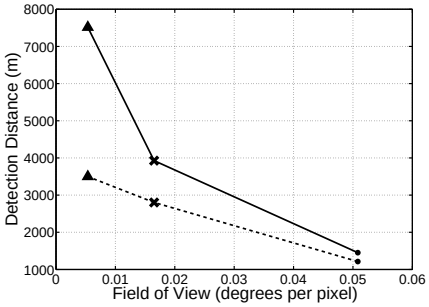

Fig. 2 Detection distance versus camera field-of-view at 50dB average detection confidence level (solid line) and 100dB average detection confidence level (dashed line). The triangle, cross, and circle markers correspond to lenses HF50HA-1B, M1614-MP, and H0514-MP, respectively.

tection distance at 50dB and 100dB average detection confidence levels (solid and dashed lines, respectively). A smaller degrees/pixel FOV is required to detect targets at greater distances with the same level of confidence (moving right to left along curve). Alternatively, for a fixed FOV, the cost to detect with a higher level of confidence is a reduction in detection range (moving vertically from top to bottom curve).

Figure 3 consists of zoomed in 160-by-80 pixel images illustrating the appearance of the target Cessna aircraft at the distances corresponding to the 50dB average detection confidence level (left column) and 100dB average detection confidence level (right column) for lenses H0514-MP (top row), M1614-MP (middle row), and HF50HA-1B (bottom row). We observe that in general, a more distinct target is required to achieve a higher level of detection confidence. We observe that as the lens degrees/pixel FOV is reduced (i.e. looking at images from top to bottom), more detail can be perceived despite increased distances to the target aircraft , hence allowing say the HF50HA-1B lens to detect with the same confidence level but at greater ranges than the other two lenses.

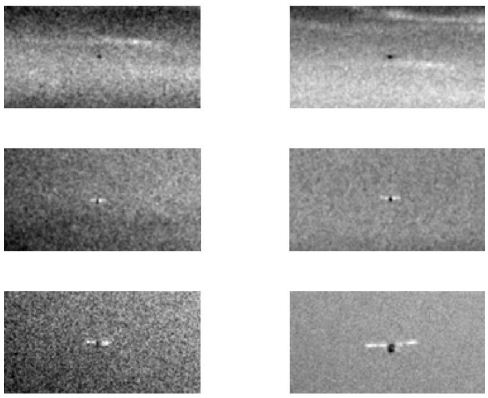

Fig. 3 Contrast enhanced images of target Cessna aircraft at 50dB average detection confidence level (left column) and 100dB average detection confidence level (right column). The top, middle, and bottom rows correspond to images taken with the H0514-MP, M1614-MP, and HF50HA-1B lenses, respectively.

4.2 Detection Distance verses False Alarm Tradeoffs

Figure 4 illustrates the growth in the ΔDSNR statistic (higher values correspond to higher detection confidence) related to the detection output from the M1614-MP lens (other lens types exhibited similar trends). Here, the average ΔDSNR value is based on ΔDSNR values averaged over 10 consecutive frames. The crosses mark the two M1614-MP lens data points used in Figure 2. One common accepted way to describe the trade-off between two competing performance quantities is through the used of a receiver or system operating characteristic curves.

Figure 5 shows a receiver operating characteristic (ROC) curve that illustrates the trade-off between detection distance and false alarm performance for the M1614-MP lens. We highlight that with higher detection thresholds (i.e. moving right to left along the curve) the incidence of false alarms is reduced but so is the detection range. The maximum detection distance at which no false alarms were triggered is approximately 2400m.

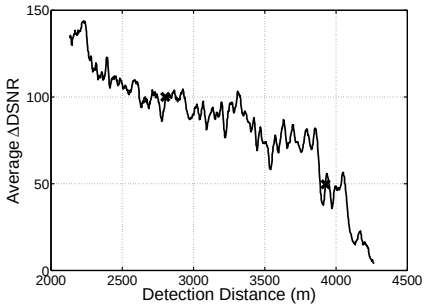

Fig. 4 Evolution of average ΔDSNR (detection confidence) for 1.65×10^{-2} degrees/pixel field-of-view lens (M1614-MP). The crosses indicate the two data points in Figure 2 corresponding to lens M1614-MP.

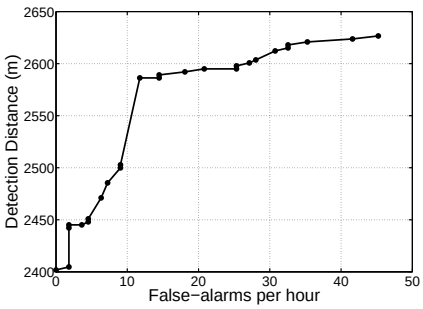

Fig. 5 Detection distance versus false alarm performance for M1614-MP lens.

Intuitively, the growth of average ΔDSNR value with decreasing range describes the fundamental nature of the trade-off between detection distance and false alarm susceptibility. For example, if wait until the average ΔDSNR gets to 110-120dB, we can expect to detect the target at around 2500m (based on Figure 4) and incur a false alarm rate of about 9/hour (based on Figure 5) if using the M1614-MP lens. Alternatively, we could attempt to ensure earlier detection of the target, at longer ranges, on the basis of a lower ΔDSNR value, but with the disadvantage of higher false alarm susceptibility. Earlier (or longer range) detection is desirable because it corresponds to greater opportunity to execute corrective action and avoid collision. Yet, we want to minimize unnecessarily executing avoidance actions, and hence minimize false-alarm susceptibility.

5 Conclusion

In this paper, we presented survey of vision-based aircraft detection approaches. We also performed an analysis of the critical system design trade-offs of: field-of-view, detection range, and false alarm performance. We identified a number of practical issues such as false targets arising from cloud backgrounds and compensation for platform vibrations and aero-dynamic disturbances.

The analysis presented showed that reducing sensor field-of-view (whilst maintaining image resolution) leads to larger detection ranges (for similar false-alarm rates). Although this observation might seem straightforward, the relationship between detection confidence level, field-of-view choice, detection range and false alarm rate is not.

Acknowledgement

This research was supported under Australian Research Council's Linkage Projects funding scheme (project number LP100100302) and the Smart Skies Project, which is funded, in part, by the Queensland State Government Smart State Funding Scheme.

References

[1] R. Carnie, R. Walker, and P. Corke, "Image processing algorithms for UAV "sense and avoid"," in *Proc. IEEE International Conference on Robotics and Automation (ICRA)*, Orlando, FL, 2006.

[2] J. Lai, J. J. Ford, P. O'Shea, R. Walker, and M. Bosse, "A study of morphological pre-processing approaches for track-before-detect dim target detection," in *Proc. Australasian Conference on Robotics and Automation (ACRA)*, Canberra, 2008.

[3] J. Lai, J. J. Ford, P. O'Shea, and R. Walker, "Hidden Markov model filter banks for dim target detection from image sequences," in *Proc.*

Digital Image Computing: Techniques and Applications (DICTA), Canberra, 2008.

[4] J. Lai and J. J. Ford, "Relative entropy rate based multiple hidden Markov model approximation," *IEEE Trans. Signal Process.*, vol. 58, pp. 165–174, 2010.

[5] L. Mejias, J. Ford, J. Lai, "Towards the Implementation of Vision-Based UAS Sense and Avoid System", *Proc. of 27th ICAS CONGRESS*, Nice, France, 19 - 24 September 2010.

[6] Luis Mejias and Scott McNamara and John Lai and Jason Ford, "Vision-Based Detection and Tracking of Aerial Targets for UAV Collision Avoidance", *Proc. of IEEE/RSJ International Conference on Intelligent Robots and Systems*, 18-22 October 2010, Taipei International Convention Center, Taipei.

[7] J. Lai, L. Mejias, and J. J. Ford, "Airborne vision-based collision-detection system," *Journal of Field Robotics*, vol. 28, pp. 137–157, 2011.

[8] R. Clothier, R. Walker, R. Baumeister, M. Brunig, J. Roberts, A. Duggan, and M. Wilson, "The smart skies project," *IEEE Aerosp. Electron. Syst. Mag.*, vol. 26, pp. 14–23, 2011.

[9] John Lai, Jason J Ford, Luis Mejias, Peter O'Shea and Rod Walker, "Detection versus False Alarm Characterisation of a Vision-Based Airborne Dim-Target Collision Detection System", in *Proc. of International Conference on Digital Image Computing: Techniques and Applications (DICTA)*, Dec. 2011.

[10] A. Wainwright, J. J. Ford, and J. Lai, "Fat and Thin Adaptive HMM Filters for Vision based Target Detection", in *Proc of Australasian Conference on Robotics and Automation (ACRA)*, Melbourne, 2011.

[11] L. Mejias, J.S. Lai, J.J. Ford, & P.J. O'Shea, "Demonstration of closed-loop airborne sense-and-avoid using machine vision" (In Press) *IEEE Aerospace and Electronic Systems Magazine*, 2012.

[12] Mejias, Luis, Ford, Jason J., & Lai, John S."Flight Trial of an Electro-Optical Sense-and-Avoid System". *Proceedings of the 28th International Congress of the Aeronautical Sciences (ICAS 2012)*, International Congress of the Aeronautical Sciences, Brisbane, Australia, 2012.

[13] J. Lai, Jason Ford, Peter O'Shea, Luis Mejias, & Rod Walker, See and Avoid Using Onboard Computer Vision" book chapter in P. Angelov (Ed) "Sense and Avoid in UAS", (In Press) John Wiley, ,2012.

[14] "Limitations of the see-and-avoid principle," Australian Transport Safety Bureau, Australian Government, Tech. Rep., 1991.

[15] Federal Aviation Administration, U.S. Department of Transportation, Tech. Rep. AC 90-48C, 1983.

[16] "Unmanned aircraft systems roadmap 2007–2032," Office of the Secretary of Defense, Department of Defense, Tech. Rep., 2007.

[17] M. T. DeGarmo, "Issues concerning integration of unmanned aerial vehicles in civil airspace," The MITRE Corporation, Tech. Rep. MP 04W0000323, 2004.

[18] B. Karhoff, J. Limb, S. Oravsky, and A. Shephard, "Eyes in the domestic sky: An assessment of sense and avoid technology for the army's "warrior" unmanned aerial vehicle," in *Proc. IEEE Systems and Information Engineering Design Symposium (SIEDS)*, Charlottesville, VA, 2006.

[19] D. Dey, C. Geyer, S. Singh, and M. Digioia, "Passive, long range detection of aircraft: Towards a field deployable sense and avoid system," in *Proc. Field and Service Robotics*, Cambridge, MA, 2009.

[20] C. Geyer, D. Dey, and S. Singh, "Prototype sense-and-avoid system for UAVs," Robotics Institute, Carnegie Mellon University, Tech. Rep. CMU-RI-TR-09-09, 2009.

[21] J. Utt, J. McCalmont, and M. Deschenes, "Development of a sense and avoid system," in *Proc. AIAA Infotech*, Arlington, VA, 2005.

[22] Z. Xiao, M. Xingang, and Z. Guilin, "Second order morphology algorithm for IR small target enhancement in sea clutter background," in *Proc. International Conference on Optics Photonics and Energy Engineering (OPEE)*, Wuhan, China, 2010.

[23] T. Gandhi, M.-T. Yang, R. Kasturi, O. Camps, L. Coraor, and J. McCandless, "Detection of obstacles in the flight path of an aircraft," *IEEE*

Trans. Aerosp. Electron. Syst., vol. 39, pp. 176–191, 2003.

[24] J. McCalmont, J. Utt, M. Deschenes, M. Taylor, R. Sanderson, J. Montgomery, R. S. Johnson, and D. McDermott, "Sense and avoid technology for unmanned aircraft systems," Proc. SPIE 2007. doi:10.1117/12.720867

[25] J. Utt, J. McCalmont, and M. Deschenes, "Test and integration of a detect and avoid system," in Proceedings of AIAA Infotech, Chicago, IL, 2004.

[26] J. F. McCalmont, "Sense and avoid technology for global hawk and predator UAVs," pp. 684–692, 2005.

[27] J. W. McCandless, "Detection of aircraft in video sequences using a predictive optical flow algorithm," *Optical Engineering*, vol. 38, no. 3, pp. 523+, 1999.

[28] S. Petridis, C. Geyer, and S. Singh, "Learning to detect aircraft at low resolutions," pp. 474–483, 2008.

[29] M. Kalloniatis and C.Luu, "Visual Acuity". in *Webvision: The Organization of the Retina and Visual System* H. Kolb, E. Fernandez, and R. Nelson, Salt Lake City (UT): University of Utah Health Sciences Center; 1995. Available: http://www.ncbi.nlm.nih.gov/pubmed/21413375, accessed 28 July 2011.

[30] R. J. Kephart and M. S. Braasch, "See-and-avoid comparison of performance in manned and remotely piloted aircraft," *Aerospace and Electronic Systems Magazine, IEEE*, vol. 25, no. 5, pp. 36–42, May 2010.

5.1 Copyright Statement